Simulation of high energy emission from gamma-ray bursts

Houri Ziaeepour, *Max Planck Institut für Extraterrestrische Physik (MPE), Giessenbachstraβe 1, 85748 Garching, Germany.*

Abstract

Gamma-Ray Bursts (GRBs) are the must violent explosions after the Big-Bang. Their high energy radiation can potentially carry information about the most inner part of the accretion disk of a collapsing star, ionize the surrounding material in the host galaxy and thereby influence the process of star formation specially in the dense environment at high redshifts. They can also have a significant contribution in the formation of high energy cosmic-rays. Here we present new simulations of GRBs according to a dynamically consistent relativistic shock model for the prompt emission, with or without the presence of an magnetic field. They show that the properties of observed bursts are well reproduced by this model up to GeV energies. They help to better understand GRB phenomenon, and provide an insight into characteristics of relativistic jets and particle acceleration which cannot yet be simulated with enough precision from first principles.

1 Introduction

The history of observation of exploding stars goes back quite a long time to 185 AD [Zhao, *et al.*2006]. From this observations we have learned that the life of massive and intermediate mass stars - with a mass close or slightly higher than the Sun - ends with violent explosions, generally called supernovae. The progenitor of supernovae are divided to two main groups [da Silva 1993]: Old white dwarfs which arrive to a critical mass - Chandrasekhar limit about $1.38M_\odot$ - by accretion of material from a companion (type Ia), and very massive young stars that collapse on themselves and depending on absence or presence of hydrogen line in their spectrum, are classified as type Ib/c or type II.

Since 1960 spy satellites called *Vela* designed to detect x-ray, gamma-ray, and neutron from space and atmospheric nuclear tests observed flashes of gamma-ray of extra-solar system origin [Klebesadel *et al.*1973, Bonnell 1995]. Distribution of their duration shows a clear grouping of bursts to short with duration $\lesssim 2$ sec and long with duration $\gtrsim 2$ sec. Their occurrence at cosmological distance and their association to supernovae and explosion of stars was first suggested in 1986 by B. Paczynski [Paczynski 1986]. The short bursts are believed to have been generated in the collision of compact objects such as two neutron stars or a neutron star and a black holes, and long bursts in the core collapse of massive stars.

Motivated by the absence of detection in other wavelengths and by compactness of the source (see e.g. [Piran 1999]), a *fireball* of strongly interacting $e^\pm$ plasma ejected during the explosion has been suggested as the origin of these Gamma-Ray Bursts (GRBs) [Paczynski 1986, Goodman 1986]. In this model the annihilation of $e^\pm$ to photons is assumed to be the origin of detected gamma-ray emission. But this model has various problems. For instance, it is difficult if not impossible to explain the Fast Rise Exponential Decline (FRED) shape of the peaks, their randomness, and long-lasting afterglow which has been observed since 1998 for majority of bursts, thanks to angular resolution new gamma-ray telescopes such as BATSE, Swift, and Fermi, multi-wavelength detectors on board of the Swift and Fermi satellites, and fast slew ability of ground based telescopes. Also it cannot explain the power-law spectrum of observed bursts and the lack of a thermal emission with a temperature ~ 1 MeV.

In the internal shock model, Synchrotron Self-Compton (SSC) emission produced by collisions between shells inside a relativistic ejecta are considered to be the origin of observed prompt gamma-ray [Rees & Mészáros 1994]. Similarly, the afterglow in lower energies is assumed to be produced by the collision of the remnant of the jet with circumburst material or the Inter-Stellar Material (ISM). Other models such as a flow of magnetized plasma - a Poynting flow - is another popular model for

GRBs [Lyutikov & Blandford 2003]. In this context the gamma-ray is emitted by electrons accelerated by reconnection of magnetic field lines. Variants and combination of these models are also suggested by various authors to solve some of the short comings of these models.

None of these models is completely flawless. As mentioned above the spectrum of GRBs is not consistent with a close to thermal spectrum predicted by a standard fireball model. The Poynting flow model cannot explain in a natural way the fast variation of GRB emission because the frequency of reconnection is expected to be very low. SSC that is the most favorite model of GRB emission has also various issues: To have a sufficiently hard emission the magnetic field must be significant such that the emission from most popular electrons with a Lorentz factor close to the minimum γ_m that make of the peak of spectrum be enough hard. This makes the duration of emission of single electrons very short and is known as fast cooling problem. Therefore it seems that SSC is not able to sustain long bursts. More seriously, synchrotron theory predicts a spectrum index $\alpha \sim -4/3$ at $E \ll E_{peak}$ [**?**], but observations show softer distribution with $\alpha \gtrsim -1$ at lower wing is observed. [Sakamoto *et al.*2008]. Recently, observations by the Fermi satellite up to energies ~ 100 GeV have detected a high energy component in both short and long bursts that is delayed by up to few tens of seconds in long bursts from $E \sim 100$ MeV component. It fades much slower than lower energies. Finally, SSC has a small efficiency. Particle In Cell (PIC) simulations show that only $\lesssim 10\%$ of the total kinetic energy is transfer to electrons [Spitkovsky 2008].

At present PIC simulations are not yet able to simulate GRB emission from first principles. In this proceedings we review an approximate but realistic formulation of SSC in the context of relativistic shocks model [Ziaeepour 2009a, Ziaeepour 2009b, Ziaeepour & Gardner 2011]. The aim of this exercise has been to see if despite issues discussed above internal shock-SSC model can explain observations. We also extend the model by considering an external precessing magnetic field to explain coherent oscillations observed in GRB 090709A and with less significance in other bursts. Then we present light curves and spectra of a number of simulated bursts according to this approximation. We show that due to rapid variation of physical quantities, even in presence of a precessing field, little evidence of coherent oscillation is imprinted in the emission. This explains the lack of observation of a significant oscillatory component in the light curves of GRBs. In this proceedings we present a summary of physical processes and motivations of the approximations and parameters used in our model, as well as its formulation. Details can be found in [Ziaeepour 2009a, Ziaeepour & Gardner 2011].

2 Synchrotron emission by relativistic shocks

In the framework of internal shock model, collisions between shells of material with different densities and velocities ejected by a central source produce mildly relativistic shocks. They are assumed to be cold and baryon dominated. Apriori there is no reason why faster shells should be ejected later, nonetheless velocity segregation can be automatically generated by deceleration of the front shells when they interact with surrounding material specially in Wolf-Rayet (WR) stars - the candidate progenitor of long GRBs [Fenimore & Ramirez-Ruiz 1999]. Weak precursors observed in many bursts can be due to this process [Umeda *et al.*2005].

During a collision compression of the particles behind the shock front and turbulence create transverse electric and magnetic fields and produce what is called Electromagnetic Energy Structure (EES) - a solitinic electromagnetic wave across the shock front. Particles of the slow shell fall along a helical path into the shock front and are accelerated by this field and by the short range random fields through Fermi processes. However, their penetration distance in the fast shell (upstream) is very short and they are reflected to down stream. During this deceleration they emit a fraction of their kinetic energy due to the presence of the shock induced magnetic field. The presence of an external magnetic field both helps the acceleration of electrons [Murphy *et al.*2010] and as we see below the emission of synchrotron radiation. This process is continuous i.e. electrons move back and forth across the shocked zone and in this way, dissipate the kinetic energy of the fast shell through synchrotron emission in places where

the induced magnetic field is strong and transversal. There is phase shift in the EES between electric and magnetic field. Its presence is crucial for SSC process in general, and for understanding the origin of high energy delayed tail in particular. The lifetime this acceleration-dissipation process is short because in a neutral plasma for each electron that falls to the shock front, one or more baryons - protons and neutrons - which are more massive fall too. For an observer in the rest frame of the slow shell the absorption of these baryons by the fast shell slow it down, reduces the discontinuity - the shock - and the strength of EES. We do not consider a significant internal energy for the shells and assume that the turbulence and mixing transfer the energy from fast shell to slow shell by elastic scattering. In this sense the collision is radiative, i.e. all the energy excess is radiated out.

One can distinguish two *shocked zone* in the opposite side of the initial discontinuity. If the velocity of massive particles - presumably baryons - are reduced to relativistic sound speed in the upstream, a secondary *reverse shock* front will form which propagates in the opposite direction of the main *forward shock*. Although it was expected that the difference between the dominant synchrotron frequency and time evolution of emission from forward and reverse shocks make their separation possible, multi-band and early observations of GRBs have shown the contrary. Therefore in the present approximation we only consider one radiation emitting region and call it *the active region*. Note that what we call active region does not correspond to shocked material. In particular, its width initially increases to a peak value, then declines and at the end of the collision i.e. when the two shells are coalesced, it disappears. This is in contrast of shocked region which increases monotonically until shells are completely mixed.

To simplify the model further, we also assume that the thickness of this emitting region is small, i.e. the propagation time of photons in this region is smaller than time resolution of this model. In fact for objects moving with ultra relativistic speeds with respect to a far observer, time and distance are approximately proportional: $r'(t') = \beta'(t)ct' \approx ct'$.[1] Under these approximations evolving quantities only depend on the average distance of the active region from central engine. Mathematically, this approximation is equivalent to assuming a wavelike behaviour for dynamical quantities i.e they depend on $r' - c\beta' t'$ rather than r' and t' separately. When $\beta' = const$, i.e. when there is no collision or dissipation, this is an exact solution. In this case the solution at every point can be obtained from the solution of one point.

In the standard treatment of SSC models [Rees & Mészáros 1994, Sari *et al.*1996] a simple power-law distribution is assumed for the Lorentz factor of accelerated electrons $n'_e(\gamma_e) = N_e(\gamma_e/\gamma_m)^{-(p+1)}$ for $\gamma_e \geqslant \gamma_m$. The parameters used for the phenomenological modeling of the shock and SSC emission such as fractions of total kinetic energy transferred to accelerated electrons ϵ_e and to a transversal magnetic field ϵ_B are also considered to be fixed. However, in a phenomenon as fast evolving as a GRB these assumptions do not seem realistic. For this reason in our formulation it is assumed that ϵ_e, ϵ_B, and densities evolve with time. We also consider shorter distances for the collision between shells in the range of $\sim 10^{10} - 10^{12}$ cm rather than $\gtrsim 10^{14}$ cm considered in the literature. This leads to short lags between energy bands consistent with observations. The motivation for this choice is the detection of variabilities up to the shortest time resolution of present instruments - $\sim 10^{-3}$ sec - and the association of anisotropies to the accretion disk around the forming compact object, presumably a black hole or neutron star, in the center of the collapsing star.

As for the external magnetic field, it can have various origins: a precessing Poynting flow, magnetic field frozen in the plasma, the magnetic field of the central engine or its accretion disk, and the dynamo field of the envelop if it is not completely interrupted by the explosion. Evidently a combination of all these cases can be present. For this reason and also because our simple model cannot distinguish between these field, we do not specify the origin of the magnetic field in the mathematical formulation or in the simulations, and simply consider a precessing external field i.e. a field with an origin other than the shock.

[1] Through this work quantities with a prime are measured with respect to the rest frame of the slow shell and without prime with respect to a far observer at the redshift of the central engine. Parameters do not have a prime even when the parametrization is in the slow shell frame.

We have also inspired by findings of PIC simulations and use them as input and/or motivation in the choices of parameters and distributions. For instance, simulations of relativistic shocks of $e^{\pm}$ plasma show that the distribution of accelerated electrons is close to a power-law with exponential cutoff $n'_e(\gamma_e) = N_e(\gamma_e/\gamma_m)^{-(p+1)}exp(-\gamma_e/\gamma_{cut})$ or a broken power-law [Spitkovsky 2008]. We also use the penetration distance of accelerated electrons in the slow shell $\lesssim \mathcal{O}(1) \times 10^3 \lambda_{ep}$, where λ_{ep} is plasma wavelength of electrons, in the calculation of Inverse Compton (IC) scattering of photons. This quantity is crucial because if we assume the same density in the whole slow shell, most of the photons would be scattered before they can leave colliding shells, leading to significant deviation of their spectrum from power-law with break expected from synchrotron emission and creates a double peak spectrum, in contradiction with observations.

3 Formulation

Conservation of energy and momentum determines the evolution of the shock. The velocity β' of the fast shell/active region decreases due to absorption of particles from slow shell and dissipation of kinetic energy as radiation due to synchrotron and self-Compton interactions. After a variable change the dynamic equations - energy-momentum conservation equations - for the active region can be written as:

$$\frac{d(r'^2 n' \Delta r' \gamma')}{dr'} = \gamma' \left(r'^2 \frac{d(n'\Delta r')}{dr'} + 2r'(n'\Delta r') \right) + r'^2 (n'\Delta r') \frac{d\gamma'}{dr'} = n'_0(r) r'^2 - \frac{dE'_{sy}}{4\pi m c^2 dr'} \quad (1)$$

$$\frac{d(r'^2 n' \Delta r' \gamma' \beta')}{dr'} = \beta'\gamma' (r'^2 \frac{d(n'\Delta r')}{dr'} + 2r'(n'\Delta r')) + r'^2 (n'\Delta r') \frac{d(\beta'\gamma')}{dr'} = -\frac{dE'_{sy}}{4\pi m c^2 dr'} \quad (2)$$

where r' is the average distance of the active region from central engine, n' is the baryon number density of the fast shell measured in the slow shell frame, n'_0 is the baryon number density of the slow shell in its rest frame and in general it depends on r'. Here we assume that $n'_0(r') = N'_0(r'/r'_0)^{-\kappa}$. For the ISM or thin shells where density difference across them is negligible $\kappa = 0$, i.e. no radial dependence. For a wind surrounding the central engine $\kappa = 2$. If we neglect the transverse expansion of the jet, for a thin shell/jet expanding adiabatically $\kappa = 2$ too. If the lifetime of the collision is short we can neglect the density change due to expansion during the collision and assume $\kappa = 0$. $\Delta r'$ is the thickness of the active region, γ' is the Lorentz factor of the fast shell with respect to the slow shell, $\beta' = \sqrt{\gamma'^2 - 1}/\gamma'$, $m = m_p + m_e \approx m_p$, E'_{sy} is the total emitted energy, and c is the speed of light. The evolution of the average radius of the shell is:

$$r'(t') - r'(t'_0) = c \int_{t'_0}^{t'} \beta'(t'') dt'' \quad (3)$$

where the initial time t'_0 is considered to be the beginning of the collision. Equations (1) and (2) can be solved exactly for the column density of the active region $n'(r')\Delta(r')$, but $\beta'(r')$ does not have an analytical solution. We use an iterative technique which allow to determine the solution as a function of the *coupling* defined as:

$$\mathcal{A} \equiv \frac{4\alpha m_p^2 \sigma_T n'_0 \Delta r'(r'_0) \epsilon_e^2(r'_0) \epsilon_B(r'_0)}{3m_e^2} \quad (4)$$

In presence of an external magnetic field a second interaction term is also present which its *coupling* can be defined as:

$$\mathcal{A}_1 \equiv \frac{\alpha m_p \sigma_T \Delta r'(r'_0) \epsilon_e^2(r'_0) B'^2_{ex\perp}(r'_0)}{6\pi c^2 m_e^2} \quad (5)$$

Details of this calculation is described in [Ziaeepour 2009a, Ziaeepour & Gardner 2011]

For the determination of synchrotron flux we use textbook formulations. Nonetheless, we have to integrate over angular distribution of emission for the observer. Notably, we must take into account

the fact that due to relativistic effects even the emission from a spherical shell seems highly collimated at far distances. The angle of collimation is $\sim 1/2\Gamma(r)$ where $\Gamma(r)$ is the Lorentz factor of the active region. The details of this calculation is discussed [Ziaeepour 2009a]. Finally, after integration over emission angle the expression for the received synchrotron flux is:

$$\frac{dP}{\omega d\omega} = \frac{4\sqrt{3}e^2}{3\pi} r^2 \frac{\Delta r}{\Gamma(r)} \int_{\gamma_m}^{\infty} d\gamma_e n'_e(\gamma_e) \gamma_e^{-2} K_{2/3}(\frac{\omega'}{\omega'_c}) + \mathcal{F}(\omega, r) \tag{6}$$

where $\mathcal{F}(\omega, r)$ includes subdominant terms and terms depending on the curvature of the emission surface. In [Ziaeepour 2009a] it is argued that these terms are much smaller than the dominant term, thus we neglect them in the simulations.

The advantage of the approximation presented here is that one can use the approximate analytical solutions to study the effect of various parameters and quantities on the evolution of dynamics of the ejecta and its synchrotron emission. However, the price to pay for this simplification is that we cannot determine the evolution of $\Delta r'(r')$ from first principles and must consider a phenomenological model for it. In our simulations we have used following phenomenological expressions:

$$\Delta r' = \Delta r'_\infty \left[1 - \left(\frac{r'}{r'_0}\right)^{-\delta}\right] \Theta(r' - r'_0) \quad \text{Steady state model} \tag{7}$$

$$\Delta r' = \Delta r_\infty \left[1 - \exp(-\delta' \frac{r'}{r'_0})\right] \Theta(r - r'_0) \quad \text{Exponential model} \tag{8}$$

$$\Delta r' = \Delta r'_0 \left(\frac{\gamma'_0 \beta'}{\beta'_0 \gamma'}\right)^{\tau} \Theta(r' - r'_0) \quad \text{dynamical model} \tag{9}$$

$$\Delta r' = \Delta r'_0 \left(\frac{r'}{r'_0}\right)^{-\delta} \Theta(r' - r'_0) \quad \text{Power-law model} \tag{10}$$

$$\Delta r' = \Delta r'_0 \exp\left(-\delta' \frac{r'}{r'_0}\right) \Theta(r' - r'_0) \quad \text{Exponential decay model} \tag{11}$$

The initial width $\Delta r'(r'_0)$ in the first two models is zero, therefore they are suitable for the description of formation of an active region at the beginning of internal or external shocks. The last three models are suitable for describing more moderate growth or decline of the active region.

4 Simulations

Table 1 shows the list of parameters of this model. Due to their large number it is not possible to explore the totality of parameter space. Therefore, in this section we show a few examples of simulated light curves and spectra of GRBs. Each simulation consists of at least 3 time-intervals (regimes) during which exponents are kept constant. Moreover, each time interval corresponds to a given model for the evolution of the width of the active region. The first regime must be either steady state or exponential for in which the initial width of the active region is zero. Following regimes can be either dynamical or power-law. Matching between values of evolving quantities at the boundary of regimes assures the continuity of physical quantities.

Fig. 1 show few examples of simulated bursts without and with an external magnetic fields. It is clear that in presence of an external field the bursts are usually brighter, harder, and lags between the light curves of the various energy bands are in general smaller and more consistent with observations. Nonetheless, some simulated bursts have small lags even in absence of an external field. Therefore, its presence is not a necessary condition for the formation of a GRB. The light curves of these examples show that despite the presence of a precessing field - similar to what is seen in pulsars and magnetars - there is barely any signature of oscillation in these light curves, specially in high energy bands. Only when the duration of the burst is a few times longer than oscillation period, the precession of the field

Table 1: Parameter set of the phenomenological shock model

model	r_0 (cm)	$\frac{\Delta r'_0}{r'_0}$	p	α_p	γ_{cut}	κ	γ'_0	τ	δ	ϵ_B	α_B
ϵ_e	α_e	N'_0 (cm^{-3})	$n'\Delta r'(r'_0)\Gamma_f$ (cm^{-2})		$\lvert B\rvert$ (Gauss)	f (Hz)	α_x	phase (rad.)	$(\frac{r'}{r'_0})_{max}$		

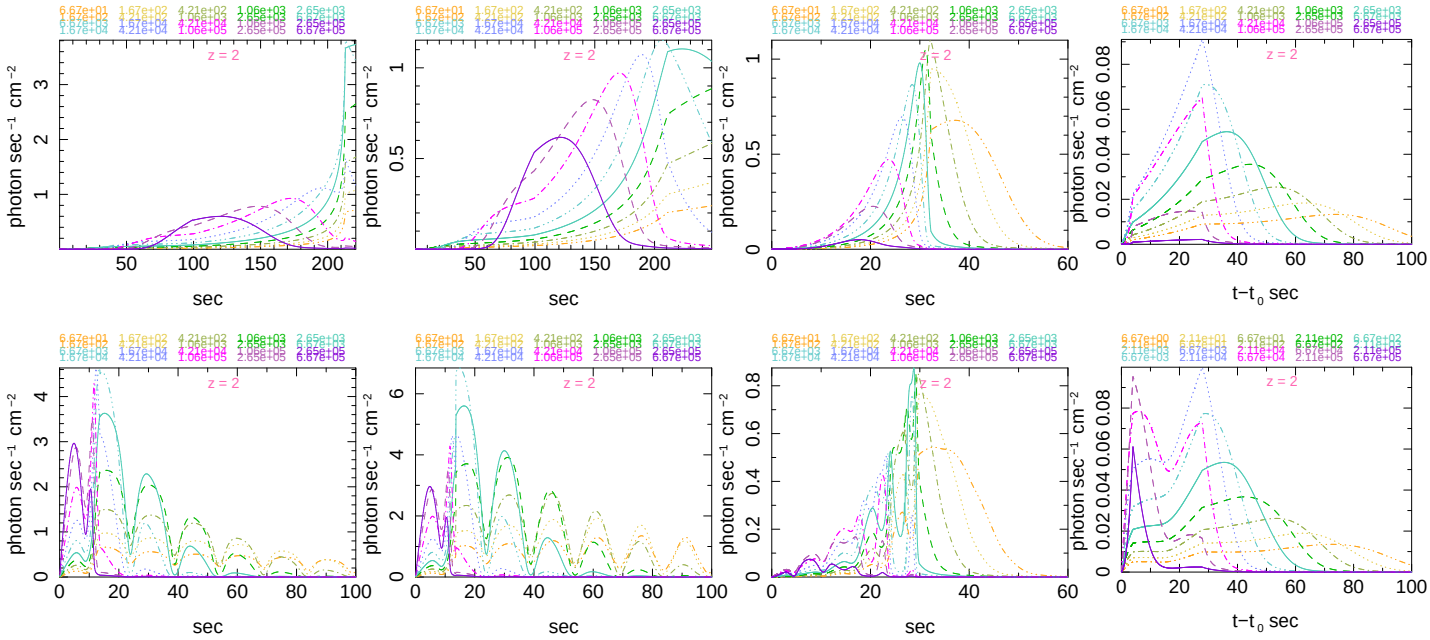

Figure 1: Top row: GRB simulations without an external magnetic field. Each simulation includes 3 regimes. The lags in the first two models from left is too large to be consistent with observations. Bottom row: Simulations with a precessing external magnetic field. From left to right: 1) $|B| = 100$ kG, $f = 0.2$ Hz 2) $|B| = 12$ kG, $f = 0.2$ Hz, and middle regime dynamical, 3) $|B| = 100$ kG, $f = 0.2$ Hz, and middle regime steady state, 4) $|B| = 2.5$ kG, $f = 0.1$ Hz. Other parameters are the same as simulations in the top row. In all plots of light curves energy bands are written on the top of the plot and the color of their font corresponds to the color of light curves of the band

creates a detectable periodic component in the light curves, see Fig. **??**. We also note that oscillations are more visible in soft X-ray and UV/optical bands. However, only in the case of the detection of a well separated precursor low energy data are available during the prompt emission. Moreover, the necessity of binning of optical data to reduce the noise can smear fast oscillations, see Fig. **??**. Therefore such oscillation can be hardly observed in real GRBs. On the other hand, in many burst e.g. GRB 070129 semi-periodic variations of the early time X-ray light curves, similar to two of the examples in Fig. 1, have been observed for a few hundreds of seconds.

Our model can be applied to both long and short bursts. An example of simulation of short bursts is shown in Fig. 2. The lags in this example is very short - consistent with observed zero lags - both in presence and absence of an external magnetic field. It also shows that very fast precession of the field can be confused with the shot noise. A remarkable properties of simulation with an external magnetic field is the presence of non-periodic substructures is the light curves from nonlinearity and fast variation of physical quantities. Fig. 3 shows some examples of spectra obtained for simulated bursts. They have a variety of behaviour at high energies. Notably, when the cutoff energy is high and the spectrum is flatter than what is possible for a simple power-law i.e. $p \leqslant 2$, the slope of the fluence at very high energies is positive, i.e. flux increases. Evidently, even in this case at very high

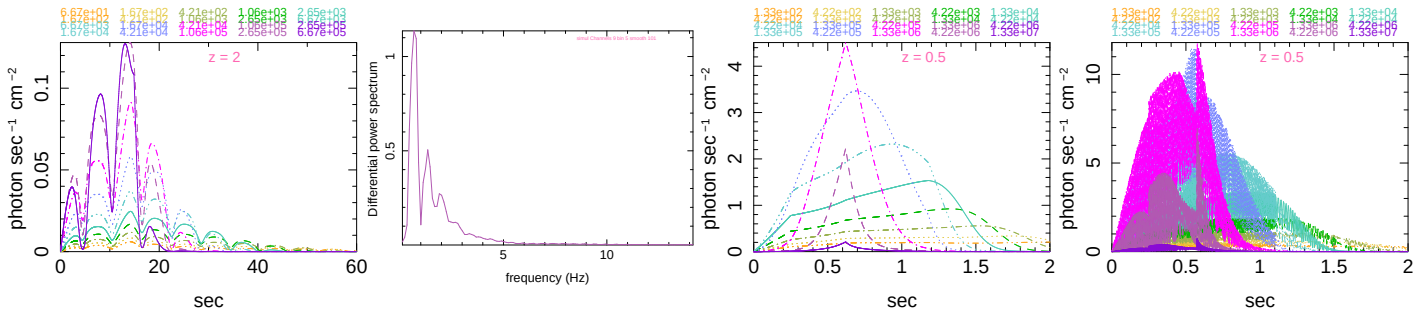

Figure 2: From left to right: 1) Simulation of a long burst with a precessing magnetic field and 2) its the Power Distribution Function (PDF) of the total light curve. Oscillatory component in high energy bands is visible by eye and in the PDF. 3,4) Simulations of a short burst without and with a fast precessing $f = 500$ Hz external magnetic field. The comparison of two plots show that due to nonlinearity of the dynamics the magnetic field induces substructures at time scales much longer than the precession period.

energies the spectrum bends and the slope becomes negative. An example of such cases is the dash-dot spectrum in the first plot of Fig. 3.

4.1 Compton scattering, delayed high energy component, and other issues

We have also simulated the effect of the inverse Compton scattering of photons by high energy electrons, but due to the limited length of this proceeding we do not show them here. As we mentioned in Sec. 2 it is crucial to consider a realistic distribution of accelerated electrons along the photons path, otherwise we overestimate the scattering rate and obtain a spectrum that is not consistent with observations. Nonetheless, the light curves of IC scattered photons are more extended in time. Thus, apriori they should explain the detected delayed emission at high energies. However their flux is much smaller then what is observed.

On the other hand, the similarity of spectra shown in Fig. 3 which include only the synchrotron emission to observations is the evidence that the origin of delayed high energy emission is the same as lower energies. In [Ziaeepour & Gardner 2011] we have given detailed arguments that the reason for the delay of high energy emission is that the most energetic electrons are trapped in the EES and follow its propagation. In fact this is a self-organizing processes: energetic electrons can follow the propagation of EES. In this way they stay in the region where electric field is strong and do not get a lag that brings them to the region where magnetic field is strong. But, because they stay longer in the high electric field region, they are accelerated more and can better follow the propagation of EES. Simple calculations show that for nominal value of parameters the delay can be tens of seconds consistent with observations. We leave a quantitative study of this process for a future work. The issues of the slope at low energies and efficiency are also discussed in [Ziaeepour & Gardner 2011] and we show that they can be explained in the context of SSC model.

References

[Zhao, *et al.*2006] Zhao FY, Strom RG, Jiang SY (2006), The Guest Star of AD185 Must Have Been a Supernova", *Chin. J. Astron. Astrophys.* **6**, (5) 635640.

[da Silva 1993] da Silva, L.A.L. (1993), The Classification of Supernovae, *Astrophys.Space.Sci.* **202**, (2) 215236.

[Klebesadel *et al.*1973] Klebesadel R.W., Strong I.B., and Olson R.A. (1973), Observations of Gamma-Ray Bursts of Cosmic Origin , *ApJ.* **182**, L85.

[Bonnell 1995] Bonnell J. (1995), http://apod.nasa.gov/htmltest/jbonnell/www/grbhist.html.

[Paczynski 1986] Paczynski, B. (1986), Gamma-ray bursters at cosmological distances, *ApJ.Lett.* **308**, (2) L43-L46.

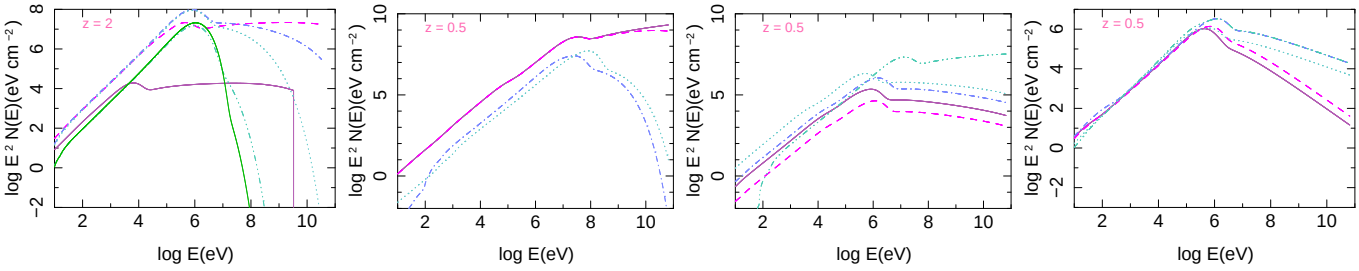

Figure 3: From left to right: 1) Electron distribution: power-law with exponential cutoff, $p = 2.5$ and $\omega_{cut}/\omega_m = 0.5$ (full line), 1 (dash-3 dots), 10 (dot), 100 (dash-dot); $p = 1.9$ and $\omega_{cut}/\omega_m = 1000$ (dash). The external magnetic field in these simulations is 10 kG. The low amplitude full line has $p = 1.9$ and $\omega_{cut}/\omega_m = 1000$ but no external magnetic field. 2) Electron distribution: power-law with exponential cutoff for electrons, $|B_{ext}| = 70$ kGauss: $\omega_{cut}/\omega_m = 1000$, $p = 1.5$ (full line); $\omega_{cut}/\omega_m = 100$, $p = 1.5$ (dash); $\omega_{cut}/\omega_m = 3$, $p = 2$ (dot-dash); $\omega_{cut}/\omega_m = 3$, $p = 2.5$ (dot). 3) Electron distribution: power-law with exponential cutoff, $|B_{ext}| = 100$ kGauss: $\omega_{cut}/\omega_m = 1000$, $p = 2.5$, $\epsilon_e = 0.002$, $\Gamma = 500$ (full line); ω_{cut}/ω_m and p as previous case and $\epsilon_e = 0.02$, $\Gamma = 50$ (dash); $n'_0 = 5 \times 10^{15}$ cm^{-3} and other parameters as the previous case (dot-dash); varying p with index -0.2, 0, 0.5, initial $p = 2.5$ and $\epsilon_e = 0.002$ (dot); initial $p = 1.8$, the same indices as previous, and $\omega_{cut}/\omega_m = 0.5$, 1000, 100 (dash-3 dots). 4) Electron distribution: broken power-law a broken slope at $\omega_{cut}/\omega_m = 3$ and $p_1 = 2.5$, $p_2 = 4$, $|B_{ext}| = 17$ kGauss (full line); $p_1 = 2.1$, $p_2 = 4$ and same $|B_{ext}|$ as previous (dash); $p_1 = 2.1$, $p_2 = 3$, $|B_{ext}| = 26$ kGauss (dot-dash); same slope and $|B_{ext}| = 35$ kGauss (dot); same slope and $|B_{ext}| = 70$ kGauss (dash-3 dots).

[Goodman 1986] Goodman, J. (1986), Are gamma-ray bursts optically thick? *ApJ.Lett.* **308**, (2) L47.

[Piran 1999] Piran, T (1999), Gamma-Ray Bursts and the Fireball Model, *Phys. Rep.* **314**, 575 [astro-ph/9810256].

[Rees & Mészáros 1994] Rees M.J. & Mészáros P. (1994), Unsteady Outflow Models for Cosmological Gamma-Ray Bursts, *ApJ.* **430**, L93 [astro-ph/9404038].

[Ziaeepour 2009a] Ziaeepour H. (2009a), Gamma Ray Bursts Cook Book I: Formulation, *MNRAS* **397**, 2009 361 [arXiv:0812.3277].

[Ziaeepour 2009b] Ziaeepour H. (2009b), Gamma Ray Bursts Cook Book II: Simulation, *MNRAS* **397**, 2009 386 [arXiv:0812.3279].

[Ziaeepour & Gardner 2011] Ziaeepour H. & Gardner B. (2011), Broad band simulation of Gamma Ray Bursts (GRB) prompt emission in presence of an external magnetic field, *J. Cosmol. Astrop. Phys.* **12**, 001.

[Fenimore & Ramirez-Ruiz 1999] Fenimore E.E. & Ramirez-Ruiz E. (1999), Gamma-Ray Bursts as internal shocks caused by deceleration, [astro-ph/9909299].

[Umeda *et al.*2005] Umeda, H., Tominaga, N., Maeda, K., & Nomoto, K. (2005), Precursors and main bursts of Gamma-Ray Bursts in a hypernova scenario, *ApJ.* **633**, 2005 L17, astro-ph/0509750.

[Medvedev & Loeb 1999] Medvedev M. & Loeb A. (1999), Generation of Magnetic Fields in the Relativistic Shock of Gamma-Ray-Burst Sources, *ApJ.* **526**, 697 [astro-ph/9904363].

[Lyutikov & Blandford 2003] Lyutikov M. & Blandford R.D. (2003), Gamma Ray Bursts as Electromagnetic Outflows, [astro-ph/0312347].

[Sari *et al.*1996] Sari R., Narayan R., & Piran T. (1996), Cooling Time Scales and Temporal Structure of Gamma-Ray Bursts, *ApJ.* **473**, 204 [astro-ph/9605005].

[Sakamoto *et al.*2008] Sakamoto T., *et al.*(2008), The First Swift BAT Gamma-Ray Burst Catalog, *ApJ.Suppl.* **175**, 179 [arXiv:0707.4626].

[Spitkovsky 2008] Spitkovsky A. (2008), Particle acceleration in relativistic collisionless shocks: Fermi process at last?, *ApJ.* **682**, 5 [arXiv:0802.3216].

[Murphy *et al.*2010] Murphy G.C., Dieckmann M.E., Drury L. O'C. (2010), Multidimensional simulations of magnetic field amplification and electron acceleration to near-energy equipartition with ions by a mildly relativistic quasi-parallel plasma collision, IEEE Transactions on Plasma science, 38, 2985 [arXiv:1011.4406].